doi: 10.15407/ujpe61.04.0283

A.M. SAVRASOV

Institute for Nuclear Research, Nat. Acad. of Sci. of Ukraine
(47, Nauky Ave., Kyiv 03680, Ukraine; e-mail: asavrasov@kinr.kiev.ua)

PACS 29.27.-a, 23.35.+g
29.30.Kv, 24.10.Lx

ISOMERIC CROSS-SECTION RATIOS FOR ^{93,95}Tc AND ^{95}Nb NUCLEI

Isomeric cross-section ratios have been measured for $^{93}Tc^{m,g}$ nuclei in the (d,n) and (p,γ) reactions, for $^{95}Tc^{m,g}$ nuclei in the (d,n) reaction, and for $^{95}Nb^{m,g}$ nuclei in the (d,α) reaction for deuterons and protons with maximum energies of about 4.5 and 6.8 MeV, respectively. Experimental values of isomeric cross-section ratios are compared with theoretical values calculated using the codes TALYS-1.4 and EMPIRE-3.2. A high influence of non-statistical effects is observed.

Keywords: isomeric ratio, activation method, γ-spectroscopy, statistical model.

1. Introduction

Nuclear reactions with various projectiles comprise an important source of information on both the mechanisms of nuclear reactions and the properties of the excited states of atomic nuclei. Information of this kind has been accumulated experimentally for many years using various methods. One of the directions of those researches is the measurement of isomeric ratios (IRs), i.e. the measurement of isomeric cross-sections ratios (ICSRs) or isomeric yield ratios (IYRs) between the reactions of formation of a final nucleus in the isomeric and ground states. Those ratios depend on the target nucleus spin and the inserted angular momentum, which is determined by the projectile mass and energy, as well as on the mechanism of a specific reaction and the properties of excited states in both continuous and discrete energy intervals [1]. Hence, the data on IRs can be used to study both the mechanisms of nuclear reactions and the statistical properties of atomic nuclei in excited states.

The obtained information is less ambiguous for simple nuclear reactions, such as (γ, n), (n, γ), (d, p), (p, γ), (d, n), and (d, α). In all those reactions, if the projectile energy is low, a small angular momentum of $(1/2\div1)\hbar$ is inserted into the nucleus, and the momentum dispersion after the particle departure changes from $\hbar$ to $2\hbar$.

Reactions with charged particles remain less studied, especially in the near-threshold interval of projectile energies. However, this is the energy interval, in which the non-statistical mechanisms and the influence of the structure of excited levels in the residual nucleus can make a substantial contribution to the population of the ground and isomeric states. Therefore, the reactions with low-energy protons and deuterons are used in our researches. In all examined residual nuclei, i.e. ^{95}Nb and ^{93,95}Tc, the isomeric and ground states have inversed spin values: the ground state is spin-up, and the isomeric one is spin-down, with the magic number $N = 50$ (^{93}Tc) is summed up with 2 (^{95}Tc) or 4 (^{95}Nb) neutrons.

At present, those nuclei have not been studied enough. For the nuclear reaction ^{92}Mo (d, n) ^{93}Tc, the numerical values of ICSRs were obtained only in two works [2, 3] (in work [2], for 4-MeV deuterons). A similar situation is observed for the reactions ^{94}Mo (d, n) ^{95}Tc and ^{92}Mo (p, γ) ^{93}Tc. The ICSRs for the first reaction were measured only in work [2] (also for 4-MeV deuterons), and for the sec-

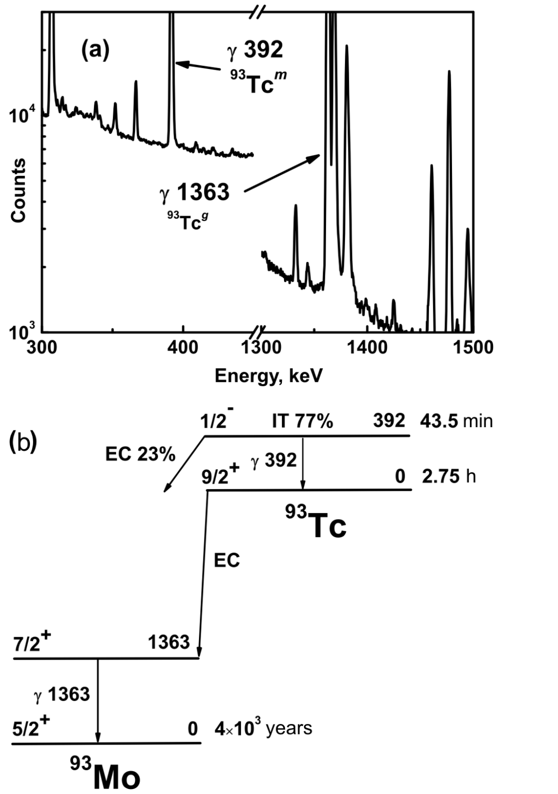

Fig. 1. Fragments of the spectrum (*a*) and decay schemes for the ^{93}Tc^{m,g} nucleus (*b*)

ond one in works [4–6] (for various proton energies). The ICSRs for the reaction ^{97}Mo (d, α) ^{95}Nb^{m,g} were not studied at all.

From all the mentioned, this work is aimed (i) at measuring the isomeric cross-section ratios for the ^{93}Tc^{m,g} nuclei in the $(\mathrm{d,n})$ and (p,γ) reactions, for the ^{95}Tc^{m,g} nuclei in the $(\mathrm{d,n})$ reaction, and for the ^{95}Nb^{m,g} nuclei in the (d,α) reaction at proton and deuteron energies of 6.8 and 4.5 MeV, respectively; (ii) at calculating theoretically the isomeric cross-section ratios for the indicated proton and deuteron energies with the help of the software packages TALYS-1.4 and EMPIRE-3.2; and (iii) at comparing the theoretical and experimental ICSR values and analyzing the mechanisms of nuclear reactions and the structure of excited levels.

2. Experimental Part

The isomeric cross-section ratios were calculated using the activation method by directly measuring the induced activity of nuclear reaction products. This technique is sensitive to the products of nuclear reactions that are characterized by a low yield and to excited low-energy isomeric levels. Since both the isomeric and ground states are formed simultaneously and under the same experimental conditions, the corresponding measurements can be performed with a high accuracy.

2.1. Specimens and irradiation procedure

Ths ISCR measurements in the (d, n) and (d, α) reactions were carried out, by using deuteron beams obtained on a tandem-generator EGP-10K at the Department of electrostatic accelerators of the Institute for Nuclear Research (INR) of the National Academy of Sciences of Ukraine. An accelerator U-120 at the Department of accelerator U-120 was used as a source of protons. The energies of deuterons and protons were equal to 4.5 and 6.8 MeV, respectively. The current was about 3 μA. Molybdenum foils with the natural isotopic composition were used as targets. They had a rectangular shape with an area of approximately 2 cm^2 and a thickness of 100 μm. Several irradiations series were performed. Specimens were irradiated for 1.5–4 h, which provided a sufficient decay activity for both the ground and isomeric states.

2.2. Activity measurement

After the irradiation, the activated specimens were transferred into a separate room with a spectroscopic installation. The gamma spectra of reaction products were measured on γ-spectrometers, which included CANBERRA and ORTEC HPGe detectors with a registration efficiency of 15–30% in comparison with the NaI(Tl) detector 3×3 in^2 in size and an energy resolution of 1.8–2 keV for γ-lines of ^{60}Co, amplifiers, and multichannel analyzers connected to computers for the information accumulation and storage.

^{93}Tc nucleus has one isomeric state, and its ground state is unstable [7]. The ^{93}Tc isomeric state has $I^\pi = 1/2^-$, and the ground one $I^\pi = 9/2^+$ [7]. In order to find the population cross-section for the isomeric level of ^{93}Tc, we determined the photopeak intensity of γ-line at 0.392 MeV, which is inherent to the decay of ^{93}Tc isomeric state only ($T_{1/2} = 43.5$ min) [7] (see Fig. 1). In order to determine the population of the ^{93}Tc ground state ($T_{1/2} = 2.75$ h), we used the γ-transition at 1363 keV that occurs after the decay of the second ^{93}Mo excited state, which is populated owing to the electron capture from the ^{93}Tc ground state only (see Fig. 1).

The ^{95}Tc nucleus has one isomeric state, and its ground state is also unstable [7]. The ^{95}Tc isomeric state has $I^{\pi} = 1/2^{-}$, and the ground one $I^{\pi} = 9/2^{+}$ [7]. In order to find the population cross-section for the isomeric level of ^{95}Tc, we determined the photopeak intensity of the γ-line at 835 keV, which is inherent to the decay of the excited ^{95}Mo level with an energy of 1039 keV, which is populated owing to the electron capture from the ^{95}Tc isomeric state only ($T_{1/2} = 61$ day) [7] (see Fig. 2). In order to determine the population of the ^{95}Tc ground state, we used the γ-transition at 766 keV from the ^{93}Mo excited state with the given excitation energy, which is populated at the electron capture from the ^{95}Tc ground state only ($T_{1/2} = 20$ h) (see Fig. 2).

^{95}Nb nucleus has one isomeric state and an unstable ground state [7]. The ^{95}Nb isomeric state has $I^{\pi} = 1/2^{-}$, and the ground one $I^{\pi} = 9/2^{+}$ [7]. In order to find the population cross-section for the iso-

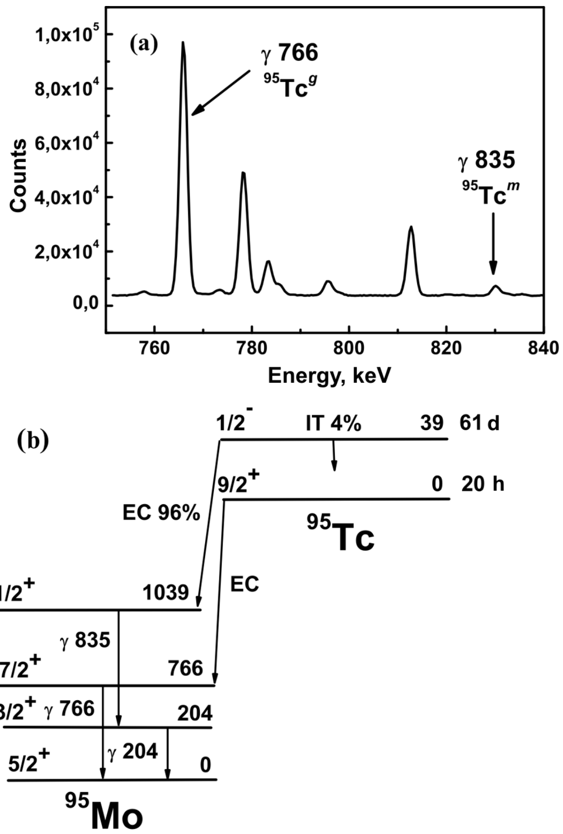

mm

Fig. 2. The same as in Fig. 1, but for the ^{95}Tc^{m,g} nucleus

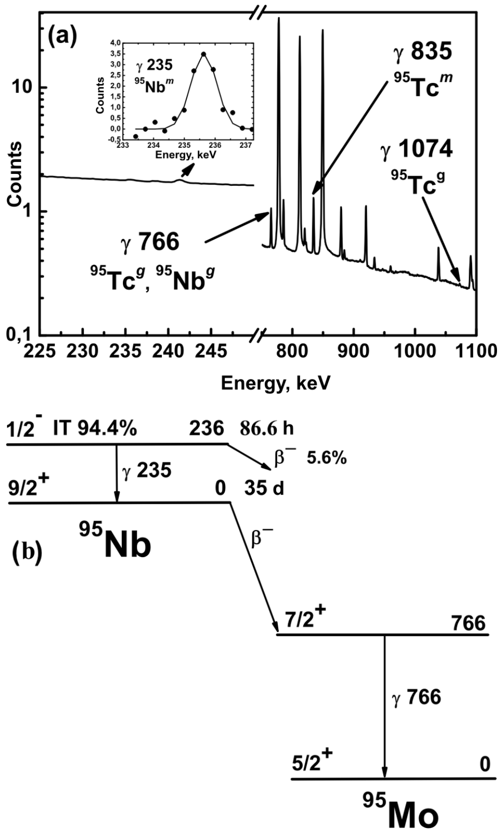

Fig. 3. The same as in Fig. 1, but for the ^{95}Nb^{m,g} nucleus

meric level of ^{95}Nb, we determined the photopeak area of the γ-line at 0.235 MeV, which is inherent to the decay of ^{95}Nb isomeric state only ($T_{1/2} = 86.6$ h) [7] (see Fig. 3). In order to determine the population of the ^{95}Nb ground state ($T_{1/2} = 35$ day), we used the γ-transition at 766 keV from the ^{93}Mo excited state with the given excitation energy, which is populated at the β-decay from the ^{95}Nb ground state only (see Fig. 3). Since this transition also accompanies the decay of ^{95}Tc^g, its contribution to the intensity of the γ-peak at 766 keV was taken into account, by using the γ-transition with an energy of 1074 keV, which is inherent to the decay of ^{95}Tc^g only and is observed with a good statistical accuracy in the γ-spectrum (see Fig. 3). The method of proportions was used at that.

3. Results

Experimental γ-spectra were used to determine the isomeric cross-section ratios $\sigma_{\rm m}/\sigma_{\rm g}$ for ^{93}Tc^{m,g},

Experimental and theoretical (model) values of isomeric cross-section ratios and model parameters: σ_h is the cross-section of high-spin level population, σ_l the cross-section of low-spin state population, E^{*1} the energy of residual nucleus excitation, E^{*2} the energy of the last discrete level of the residual nucleus used in calculations

Reaction	Energy, MeV	σ_h/σ_l			E^{1*}, MeV	E^{2*}, MeV
		Experiment	Talys-1.4	Empire-3.2		
^{92}Mo(d,n)^{93}Tc^{m,g}	4.5	1.13 ± 0.1	2.0	5.1	6.3	6.0
^{94}Mo(d,n)^{95}Tc^{m,g}	4.5	1.07 ± 0.11	2.1	3.5	7.1	2.8
^{92}Mo(p,γ)^{93}Tc^{m,g}	6.8	0.29 ± 0.03	2.0	1.6	10.9	6.0
^{97}Mo(d,α)^{95}Nb^{m,g}	4.5	3.64 ± 0.3	2.9	31	14.5	5.8*

* In the case of EMPIRE-3.2, only discrete levels with the excitation energy below the neutron binding energy in the nucleus were made allowance for. Therefore, only 57 levels were taken into consideration for ^{95}Nb nucleus.

^{95}Tc^{m,g}, and ^{95}Nb^{m,g} nuclei by the formula [8]

$$d = \frac{\sigma_{\rm m}}{\sigma_{\rm g}} = \left[\frac{\lambda_{\rm g} f_{\rm m}(t)}{\lambda_{\rm m} f_{\rm g}(t)}\left(\frac{\xi_{\rm m}k_{\rm m}\alpha_{\rm m}N_{\rm g}}{\xi_{\rm g}k_{\rm g}\alpha_{\rm g}N_{\rm m}} - \frac{p\lambda_{\rm g}}{\lambda_{\rm g}-\lambda_{\rm m}}\right) + \right. \left. + \frac{p\lambda_{\rm m}}{\lambda_{\rm g}-\lambda_{\rm m}}\right]^{-1}, \quad (1)$$

where

$$f_{\rm m}(t) = [1-\exp(-\lambda_{\rm m}t_{\rm irr})]\exp(-\lambda_{\rm m}t_{\rm cool}) \times \times [1-\exp(-\lambda_{\rm m}t_{\rm meas})], \quad (2)$$

$$f_{\rm g}(t) = [1-\exp(-\lambda_{\rm g}t_{\rm irr})]\exp(-\lambda_{\rm g}t_{\rm cool}) \times \times [1-\exp(-\lambda_{\rm g}t_{\rm meas})], \quad (3)$$

$N_{\rm g}$ and $N_{\rm m}$ are the intensities of photopeaks accompanying the decay of daughter nuclei in the isomeric (m) and ground (g) states; $\alpha_{m,g}$ are the yields of γ-quanta at the decay of the isomeric and ground states; $\xi_{m,g}$ the efficiencies of γ-quantum registration; $t_{\rm irr}$, $t_{\rm cool}$, and $t_{\rm meas}$ are the irradiation, cooling, and measurement time intervals, respectively (in seconds); $k_{m,g}$ are the self-absorption coefficients of decay γ-quanta; p is the branching coefficient (the ratio between the probability of the transition from the isomeric level on the ground one and the total probability of the isomeric level decay); and $\lambda_{\rm m}$ and $\lambda_{\rm g}$ are the decay constants of the isomeric and ground states, respectively (in s^{-1} units).

The γ-spectra were analyzed with the help of the software program Winspectrum [9]. The program makes it possible to register spectra after definite time intervals. This means that the corresponding nuclides were identified by both the energy and the half-life period. The registration efficiency of decay γ-quanta was determined in the energy interval from 32 to 1408 keV with the help of the standard calibration sources ^{133}Ba, ^{137}Cs, ^{152,154}Eu, and ^{60}Co. The calibration was tested, by using the software package GEANT4 [10], in which the calculations were carried out by applying the Monte Carlo method. The simulation results coincided with the experimental efficiency values to within the experiment error. The values for $\lambda_{\rm m}$, $\lambda_{\rm g}$, p, $k_{m,g}$, and $\alpha_{m,g}$ were taken from work [7].

The ICSR data obtained for various projectiles are quoted in Table. Other analytical lines with sufficient intensities were also used for the calculation of isomeric ratios. The values of those ratios coincide with the tabulated data within the calculation errors. The ICSR values for the reaction ^{97}Mo (d, α) ^{95}Nb^{m,g} were obtained for the first time. The data for other reactions at indicated projectile energies were also obtained for the first time.

4. Simulation and Discussion

The isomeric cross-section ratios were calculated with the use of the software packages TALYS-1.4 [11] and EMPIRE-3.2 [12]. In order to provide identical calculation conditions, 70 discrete low-energy excited levels were used in the automatic regime in both codes after compilation. Spectroscopic parameters for the levels and the schemes of their decay were taken from the library RIPL-3 [13]. In both packages, several nuclear reaction scenarios can be analyzed.

In the framework of the code TALYS-1.4 for the nuclear reactions ^{94}Mo (d, n) ^{95}Tc and ^{97}Mo (d, α) ^{95}Nb^{m,g}, the main contributions to the population cross-sections of the isomeric and ground states are given by the pre-equilibrium mechanism based on the excitonic model [14–16]. For the nuclear reactions $^{92}\mathrm{Mo}\,(\mathrm{d,n})\,^{93}\mathrm{Tc}$ and $^{92}\mathrm{Mo}\,(\mathrm{p},\gamma)\,^{93}\mathrm{Tc}$, the main contributions to the population cross-sections of the isomeric and ground states are given by the statistical mechanism based on the Hauser–Feshbach theory [17]. At the same time, in the framework of the code EMPIRE-3.2, the same statistical mechanism makes the whole contribution to the population cross-sections of the ground and isomeric level for all reactions [17].

The penetration coefficients were calculated on the basis of the spherical optical model with the help of the computer code ECIS06 [18]. The set of global parameters for neutrons and protons was taken from work [19], for deuterons from works [20, 21], and for alpha-particles from work [22]. The penetration coefficients for photons are also of great importance for the calculation of isomeric ratios. They were determined from the strength functions. In the case of TALYS-1.4, the Kopecky–Uhl Lorentzian [23] was used for the E1 transition, and the Brink–Axel function [24] for the M1, E2, and M2 ones. In EMPIRE-3.2, in the cases of E1, M1, and E2 radiation, the modified Lorentzian (model No. 1) was used [25]. The parameters for this Lorentzian were taken from the following sources: in the case of E1 transitions, from the experimental database or, in its absence, from the theoretical one [13]; for E2 radiation, from works [26, 27], and for M1 transition from work [28]. In the model EMPIRE-3.2, M2 transitions were not taken into account.

The package TALYS-1.4 includes five model variants for the description of level density, and the EMPIRE-3.2 does four ones. The choice of any of those variants is determined with the help of the following input keywords: "ldmodel" in TALYS-1.4 and "LEVDEN" in EMPIRE-3.2. At the further analysis of the simulation results obtained for the description of a level density in the continuous excitation energy interval, the model of constant temperature and Fermi gas (CT + FG) is used in both models [29]. The application of other models for the description of a level density and radiative strength functions, which were realized in both packets, did not result in a considerably better agreement between the theory and the experiment.

The isomeric ratios for the reactions $^{92}\mathrm{Mo}\,(\mathrm{d,n})\,^{93}\mathrm{Tc}^{m,g}$, $^{97}\mathrm{Mo}\,(\mathrm{d},\alpha)\,^{95}\mathrm{Nb}^{m,g}$, and

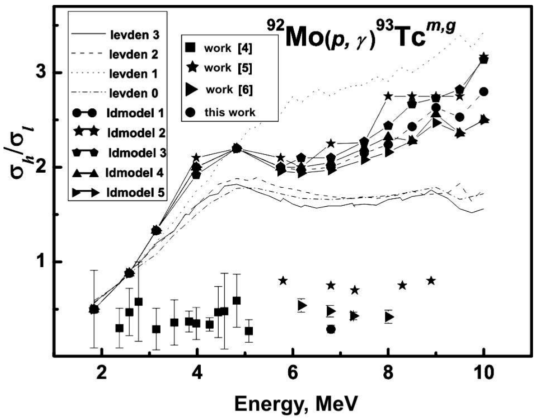

Fig. 4. Experimental and theoretical ICSRs for the nuclear reaction $^{92}\mathrm{Mo(p,}\gamma)^{93}\mathrm{Tc}^{m,g}$. To describe the level density, the following models were used: ldmodel = 1 and levden = 2 correspond to the model of constant temperature (CT) and Fermi gas (FG) (CT + FG) [29]; levden = 3 to the microscopic combinatorial model (HFBM) [30]; levden = 1 to the generalized superfluid model (GSM) [31, 32]; levden = 0 to the improved superfluid model (EGSM) [33]; ldmodel = 2 to the back-shifted Fermi gas model (BFM) [34]; ldmodel = 3 to the generalized superfluid model (GSM) [35, 36]; ldmodel = 4 to the microscopic model [37]; and ldmodel = 5 to the microscopic model [38]

$^{94}\mathrm{Mo}\,(\mathrm{d,n})\,^{95}\mathrm{Tc}^{m,g}$ were calculated theoretically in the energy interval from the threshold value to 4.5 MeV with a step of 0.5 MeV. For the reaction $^{92}\mathrm{Mo}\,(\mathrm{p},\gamma)\,^{93}\mathrm{Tc}^{m,g}$, the ICSRs were simulated at energies from the threshold value to 6.8 MeV with a step of 0.5 MeV. The results obtained give rise to the following conclusions. In the case of the $^{92}\mathrm{Mo}\,(\mathrm{p},\gamma)\,^{93}\mathrm{Tc}^{m,g}$ reaction, the ICSR values practically do not change with the growth of the proton energy and remain at the level $\sigma_h/\sigma_l = 2.0$ for TALYS-1.4 and $\sigma_h/\sigma_l = 1.6$ in the EMPIRE-3.2 case, exceeding the experimental value by approximately a factor of 6.9 or 5.5, respectively (see Table).

For this reaction, experimental data are available in a wide range of proton energies. Those experimental ICSRs together with the values of level density theoretically calculated for various models are depicted in Fig. 4. None of the used models improves the agreement between the theoretical and experimental data for the level density at proton energies from 3.0 to 8.9 MeV. However, at the lowest proton energies, the difference between the experimental and theoretical ICSRs decreases and vanishes at $E_p = 1.84$ MeV. The excitation energy of the residual nucleus at $E_p = 1.84$ MeV equals 5.94 MeV and prac-

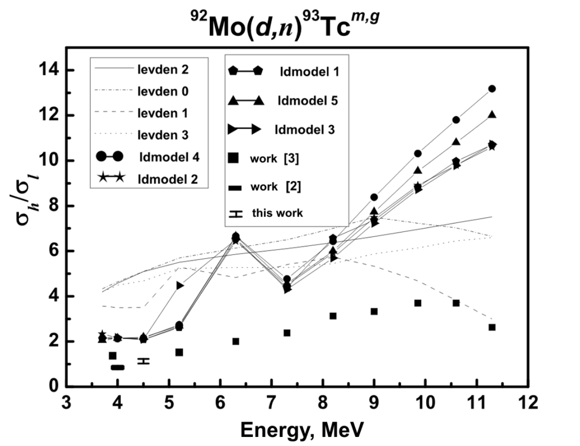

Fig. 5. The same as in Fig. 4, but for the nuclear reaction ^{92}Mo(d,n)^{93}Tc^{m,g}

tically coincides with the energy of the 70-th discrete level of ^{93}Tc.

A hypothesis can be put forward that the difference between the experimental and theoretical ICSRs may probably result from the presence of unidentified high- and low-energy γ-transitions with a low multipolarity in ^{93}Tc nuclei from the region of residual nucleus excitation energy (6.5–13 MeV) on low-energy excited levels in the discrete spectrum, with their subsequent decay onto an isomeric spin-down level of ^{93}Tc. This circumstance was not taken into consideration at the theoretical modeling. The decay scheme is also unknown for many highly excited discrete levels of ^{93}Tc, and they decay in the models onto the ground spin-up level, which also can insert an additional error.

In the case of the ^{92}Mo(d,n)^{93}Tc^{m,g} reaction, the ICSR practically does not change with the growth of the deuteron energy and remains at the level $\sigma_h/\sigma_l = 2.0$ for TALYS-1.4 and $\sigma_h/\sigma_l = 5.1$ for EMPIRE-3.2, exceeding the experimental value by approximately a factor of 1.8 or 4.5, respectively. In the code TALYS-1.4, there is a possibility to consider an increase of the contribution by direct mechanisms, namely, the stripping reactions $(\mathrm{d,n})$ [39]. However, by varying the keywords that regulate the contributions of the direct and pre-equilibrium mechanisms, we did not improve the agreement between the experimental and theoretical values for the isomeric cross-section ratios. For this reaction, there are experimental data in a wide interval of deuteron energies. Those experimental ICSRs together with the level densities theoretically calculated for various models are shown in Fig. 5. In this case, the excitation energy of the residual nucleus amounts to 5.7 MeV at a deuteron energy of 3.9 MeV, which is lower than the energy of the 70-th discrete level. However, even in the case concerned, the difference between the theoretical and experimental ICSR values is rather substantial, although it is absent in the case of (p,γ) reaction at a close excitation energy of the residual nucleus. Hence, in this case, the difference between the experimental and theoretical ICSR values at deuteron energies of 3.9–4.5 MeV can be explained by a different structure and different decay schemes of the excited levels, which are populated in the course of the $(\mathrm{d,n})$ reaction, unlike the (p,γ) one. At higher deuteron energies, the difference can also originate, as was in the case of the (p,γ) reaction, from the presence of high- and low-energy γ-transitions with a low multipolarity in ^{93}Tc nuclei from the interval of residual nucleus excitation energies (7–14 MeV) onto low-energy excited levels in the discrete spectrum, which, in turn, decay onto the isomeric level of ^{93}Tc, and from the absence of complete information concerning the decay scheme of the discrete highly excited levels of this nucleus.

A similar situation also takes place for the reaction $^{94}\mathrm{Mo}\,(\mathrm{d,n})\,^{95}\mathrm{Tc}^{m,g}$. The ICSR remains at the level $\sigma_h/\sigma_l = 2.1$ for TALYS-1.4, but, in the case of EMPIRE-3.2, $\sigma_h/\sigma_l = 3.5$, by exceeding the experimental value by approximately 2 and 3.3 times, respectively. In the case of TALYS-1.4, if the default parameters are used, the pre-equilibrium mechanism dominates [14–16], whereas the direct mechanism is not taken into account at all. As a result of taking the contribution of the pre-equilibrium mechanism into account, the results for TALYS-1.4 are in better agreement with the experiment. Therefore, the presence of high-energy γ-transitions with a low multipolarity in ^{95}Tc nuclei from the interval of the residual nucleus excitation energies (6–7 MeV) onto low-energy excited levels in the discrete spectrum with their subsequent decay onto the isomeric low-spin level of ^{95}Tc can be responsible for those discrepancies.

An even larger difference between the theoretical and experimental values for isomeric cross-section ratios for the $^{97}\mathrm{Mo}\,(\mathrm{d},\alpha)\,^{95}\mathrm{Nb}^{m,g}$ reaction takes place in the case of EMPIRE-3.2. The ICSR values for both codes practically are not changed with the growth of the deuteron energy and remain at the level $\sigma_h/\sigma_l =$

= 2.9 for TALYS-1.4 and σ_h/σ_l = 31 for EMPIRE-3.2, which is approximately 1.26 times lower than the experimental value for TALYS-1.4 and 8.5 times larger for EMPIRE-3.2. In this case, a possible origin of better results for TALYS-1.4 can be the contribution of the pre-equilibrium mechanism. It results in the escape of an alpha-particle with a higher angular momentum in comparison with the statistical mechanism, so that the residual ^{95}Nb^{m,g} nucleus has a lower angular momentum and, accordingly, a lower cross-section of spin-up ground state population. However, it is also insufficient to explain the discrepancies. Therefore, an additional inconsistency can arise owing to a certain insignificant contribution of the statistical mechanism, which increases the experimental ICSR value. It should also be taken into account that, among all studied nuclei, the decay scheme for ^{95}Nb^{m,g} was the least studied. Of 70 excited levels, which we took into consideration, the decay schemes are known experimentally only for the lowest three transitions. This circumstance can insert an additional inconsistency.

5. Conclusions

The isomeric cross-section ratios for ^{93}Tc^{m,g} nuclei in the (d, n) and (p, γ) reactions, for ^{95}Tc^{m,g} nuclei in the (d, n) reaction, and, for the first time, for ^{95}Nb^{m,g} nuclei in the (d, α) reaction have been measured for deuterons and protons with maximum energies of 4.5 and 6.8 MeV, respectively. For theoretical calculations of isomeric ratios, the software codes TALYS-1.4 and EMPIRE-3.2 were used. The theoretical values of isomeric cross-section ratios were shown to considerably exceed the experimental ones, except for the nuclear reaction ^{97}Mo (d, α) ^{95}Nb^{m,g} simulated, by using Talys-1.4. According to EMPIRE-3.2, in all nuclear reactions with default parameters, the statistical model, which is based on the Hauser–Feshbach mechanism, dominates. At the same time, according to TALYS-1.4, the statistical model makes the major contribution for the nuclear reactions ^{92}Mo (d, n) ^{93}Tc^{m,g} and ^{92}Mo (p, γ) ^{93}Tc^{m,g}, whereas the pre-equilibrium model prevails for the reactions ^{94}Mo (p, γ) ^{95}Tc^{m,g} and ^{97}Mo (d, α) ^{95}Nb^{m,g}. However, both those models badly describe experimental ICSR values, although, in general, the software package TALYS-1.4 describes the aforementioned nuclear reactions better at the examined projectile energies than EMPIRE-3 does. A general origin of the inconsistency may probably be scarce information concerning the decay schemes for highly excited discrete levels, especially for ^{95}Nb. The contributions of nonstatistical effects can be an additional origin of discrepancies at the examined projectile energies for all nuclear reactions.

The author is grateful to the staff of the cyclotron U-120 and the tandem-generator EGP-10K for providing stable and intensive beams.

1. E.A. Bogila and V.M. Kolomietz, Ukr. J. Phys. **34**, 7 (1989).
2. I.N. Vishnevsky, V.A. Zheltonozhsky, and A.N. Savrasov, in *Abstracts of the 60-th Meeting on Nuclear Spectroscopy and Nuclear Structure "Nucleus-2010", St.-Petersburg, July 6-9, 2010* (St.-Petersburg, 2010), p. 168.
3. Z. Randa, J. Inorg. Nucl. Chem. **38**, 2289 (1976).
4. E.A. Skakun, V.G. Batij, Y. N. Rakivnenko *et al.*, Yad. Fiz. **46**, 28 (1987).
5. L.Ya. Arifov, S.A. Artemova, B.S. Mazitov, and V.G. Ulanov, in *Abstracts of the 30-th Conferernce on Nuclear Spectroscopy and Nuclear Structure, Leningrad, 18-21 March 1980* (Leningrad, 1980). p. 328 (in Russian).
6. Y. Yoshirava, S. Fukushima *et al.*, Gen. Kenk. **13**, 583 (1969).
7. R.B. Firestone, *Table of Isotops* (Wiley Interscience, New York, 1996).
8. R. Vanska and R. Rieppo, Nucl. Instr. Meth. **179**, 525 (1981).
9. I.N. Vishnevsky, V.A. Zheltonozhsky, A.G. Zelinsky *et al.*, in *Collected Scientific Articles* (Institute for Nuclear Research, Kiev, 1999), p. 60.
10. S. Agstinelli *et al.*, Nucl. Instrum. Methods A **506**, 250 (2003).
11. A.J. Koning, S. Hilaire, and M.C. Duijvestijn, in *Proceedings of the International Conference on Nuclear Data for Science and Technology* (2005), p. 1154.
12. M. Herman *et al.*, Nucl. Data Sheets **108**, 2655 (2007).
13. *Handbook for Calculations of Nuclear Reaction Data: Reference Input Parameter Library*, http://www-nds.iaea.or.at/RIPL-3/.
14. A.J. Koning and M.C. Duijvestijn, Nucl. Phys. A **744**, 15 (2004).
15. H. Gruppelaar, P. Nagel, and P.E. Hodgson, Riv. Nuovo Cimento **9**, 1 (1986).
16. E. Gadioli and P.E. Hodgson, *Pre-Equilibrium Nuclear Reactions* (Oxford University Press, Oxford, 1992); W. Dilg, W. Schantl, H. Vonach, and M. Uhl, Nucl. Phys. A **217**, 269 (1973).
17. W. Hauser and H. Feshbach, Phys. Rev. **87**, 366 (1952).
18. J. Raynal, *Notes on ECIS94* (CEA Saclay Report No. CEA-N-2772, 1994).

19. A.J. Koning and J.P. Delaroche, Nucl. Phys. A **713**, 231 (2003).
20. An. Haixia and Cai Chonghai, Phys. Rev. C **73**, 054605 (2006).
21. Yinlu Han, Yuyang Shi and Shen. Qingbiao, Phys. Rev. C **74**, 044615 (2006).
22. V. Avrigeanu, P.E. Hodgson, and M. Avrigeanu, Phys. Rev. C **49**, 2136 (1994).
23. J. Kopecky and M. Uhl, Phys. Rev. C **41**, 1941 (1990).
24. D.M. Brink, Nucl. Phys. **4**, 215 (1957); P. Axel, Phys. Rev. **126**, 671 (1962).
25. V.A. Plujko, Acta Phys. Pol. B **31**, 435 (2000).
26. J. Speth and A. van de Woude, Rep. Prog. Phys. **44**, 719 (1981).
27. W.V. Prestwich, Z. Phys. A **315**, 103 (1984).
28. A. Bohr and B. Mottelson, *Nuclear Structure, Vol. 2* (Addison-Wesley, Reading, MA, 1975).
29. A. Gilbert and A.G.W. Cameron, Can. J. Phys. **43**, 1446 (1965).
30. S. Goriely, M. Samyn, and J.M. Pearson, Phys. Rev. C **75**, 064312 (2007).
31. A. V. Ignatyuk, G. N. Smirenkin, and A. S. Tishin, Sov. J. Nucl. Phys. **21**, 255 (1975).
32. A. V. Ignatyuk, in *Technical Report INDC(CCP)* (IAEA), p. 233.
33. A. D'Arrigo *et al.*, J. Phys. G **20**, 305 (1994).
34. W. Dilg, W. Schantl, H. Vonach, and M. Uhl, Nucl. Phys. A **217**, 269 (1973).
35. A.V. Ignatyuk, K.K. Istekov, and G.N. Smirenkin, Sov. J. Nucl. Phys. **29**, 450 (1979).
36. A.V. Ignatyuk, J.L. Weil, S. Raman, and S. Kahane, Phys. Rev. C **47**, 1504 (1993).
37. S. Goriely, F. Tondeur and J.M. Pearson, At. Data Nucl. Data Tables **77**, 311 (2001).
38. S. Goriely, S. Hilaire and A.J. Koning, Phys. Rev. C **78**, 064307 (2008).
39. C. Kalbach, *private communication* (2007).

Received 21.07.15.
Translated from Ukrainian by O.I. Voitenko

А.М. Саврасов

ІЗОМЕРНІ ВІДНОШЕННЯ
ПЕРЕРІЗІВ В ЯДРАХ ^{93,95}Tc ТА ^{95}Nb

Р е з ю м е

Виміряно ізомерні відношення перерізів в ядрах $^{93}\mathrm{Tc}^{m,g}$ в (d,n) і (p,γ)-реакціях, в ядрах $^{95}\mathrm{Tc}^{m,g}$ в (d,n)-реакції, в ядрах $^{95}\mathrm{Nb}^{m,g}$ в (d,α)-реакції для дейтронів та протонів з максимальними величинами енергій 4,5 МеВ і 6,8 МеВ, відповідно. Експериментальні значення ізомерних відношень перерізів порівнюються з теоретичними, розрахованими за допомогою пакетів TALYS-1.4 та EMPIRE-3.2. Спостерігається значний вплив нестатистичних ефектів.